

SAFETY AND RISK ANALYSIS CAPABILITIES OF ASTOS

S. Weikert⁽¹⁾, T. Scholz⁽²⁾, F. Cremaschi⁽³⁾

⁽¹⁾ Astos Solutions GmbH, Meitnerstr. 10, 70563 Stuttgart, Germany, Email: sven.weikert@astos.de

⁽²⁾ Astos Solutions GmbH, Meitnerstr. 10, 70563 Stuttgart, Germany, Email: thorsten.scholz@astos.de

⁽³⁾ Astos Solutions GmbH, Meitnerstr. 10, 70563 Stuttgart, Germany, Email: francesco.cremaschi@astos.de

ABSTRACT

This paper describes the analysis capabilities of ASTOS (Aerospace Trajectory Optimization Software) in the field of in-orbit and on-ground risk assessment. ASTOS is a simulation and optimization software developed by Astos Solutions for the European Space Agency. Originally designed for the optimization of ascent trajectories it is now a flexible tool for a wide range of simulation, analysis and optimization applications for space missions. The paper is split into two parts: the first part deals with on-ground risk assessment, the second with in-orbit risk.

1. INTRODUCTION

Safety of humans and assets is essential for space mission design and mission operation. All major space agencies have released safety guidelines specifying requirements for every mission type. Engineers' responsibility is to verify that given safety margins are not violated. This task is impossible without adequate tools that assess the imposed hazard probabilities.

For on-ground risk assessment ASTOS comprises modules for destructive and non-destructive re-entry simulation. These modules compute location, mass, size and final velocity of the surviving fragments. From that a safety analysis module computes casualty and fatality probability for the re-entry event using a population density model. Additionally the maximum probable loss due to the re-entry event is calculated based on the gross domestic product of the country affected by the impact. The paper details the different options available for the re-entry simulation and explains their differences, advantages and disadvantages. Simple models based on user-defined ballistic coefficients or drag coefficient tables can be used within a trajectory optimization. These models may also be used to restrict the instantaneous impact point of a launcher ascent. More sophisticated approaches containing fragmentation and explosion models are available for simulation and analysis only. The vehicle is defined by a set of primitive shapes, each with an individual size, material and mass. In the second part the conjunction analysis module of ASTOS is presented. With this module a potential collision of the simulated vehicle with an in-orbit object can be identified.

2. ON-GROUND RISK ASSESSMENT

This section deals with the risk for humans and assets due to re-entering objects. Even though the section is called on-ground risk assessment, also risk to ships and planes is considered.

The analysis of human risk due to re-entering debris consists of two parts:

- propagation of the trajectory till the impact location(s) or demise
- calculation of the associated risk and fatality

The first part is described in section 2.1, the second in section 2.2.

2.1. Re-entry simulation

ASTOS provides a multitude of distinct re-entry simulation and optimization options. Fig. 1 provides an overview on these options.

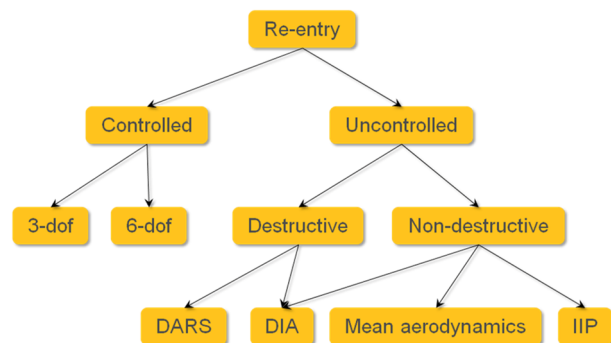


Figure 1. Tree of re-entry analysis types in ASTOS

With ASTOS it is possible to simulate and optimize controlled re-entries. The trajectory may be optimized such that the resultant reference trajectory stays in the middle of a safety corridor and that no limit of the flight envelope is exceeded. While typically three degrees of freedom (dof) are used for optimization, ASTOS comprises also 6-dof equations of motion. For uncontrolled re-entries, i.e. a satellite de-orbit, the user may select from models of different complexity. A typical application for the uncontrolled re-entry simulation is an on-ground risk assessment for which impact points need to be calculated.

In principal the re-entry analysis can be split into the following steps:

- estimation of the aerodynamics based on the current shape
- propagation of the trajectory based on aerodynamics, mass, external forces and the initial conditions
- calculation of thermal loads and heating of the vehicle
- calculation of mechanical loads
- calculation of melting
- estimation of fragmentation events
- estimation of explosion events and the resulting velocity increment

Depending on the available information and the desired computation time some of these models need to be simplified.

In early design phases the structural design of the vehicle is not fixed, therefore only a lumped mass model can be used. An analysis based on a detailed CAD model, as it is used by other tools, is therefore not possible. Also in cases where fast results are desired, the models need to be simplified since already the preparation of a detailed model needs several days or even weeks.

To avoid underestimation of the risk, any simplification should be accompanied by additional safety margins. Since there are some variables that are not exactly known, e.g. the atmospheric density, none of the existing methods can go without safety margins. These safety margins are typically applied as uncertainties within a Monte Carlo analysis. From this point of view, all the presented approaches contain a probabilistic contribution. Only when the analysis is used as a constraint for optimization problems, uncertainties are neglected since gradient based optimization algorithms need deterministic models to compute accurate finite differences. ASTOS offers several possibilities to calculate debris impacts which are described in the following.

2.1.1. Non-Destructive Re-entry

The first and simplest approach is the so-called “Combined Average Drag” or “Mean Aerodynamics” method. A user-defined aerodynamics is used to compute the re-entry trajectory. Neither melting nor breakup or explosion is considered. The result is a single impact location. The aerodynamics is defined by one of the available ASTOS aerodynamics models (see [6]), whereas the angle of attack is assumed as zero. The profile of the aerodynamic coefficients may depend on Mach number, atmospheric pressure, atmospheric density or dynamic pressure. Since this computation is very fast, it is suitable for trajectory optimization problems. Incorporated into a Monte Carlo analysis it is also a fast way to produce impact footprints, but due to the simplifying assumptions the safety margins and the footprints resulting should be relatively large. For sake of completeness, an even simpler approach shall not be

forgotten. Using the “no drag” option, the Keplerian orbit at the beginning of the re-entry is propagated until the ground. Gravitational perturbations and atmospheric effects are not considered. The output is widely referred to as the Instantaneous Impact Point (IIP). It is a good reference to check the plausibility of other re-entry analysis results.

2.1.2. Destructive Re-entry

The methods described so far do not consider any fragmentation or explosion. In this section the destructive re-entry analyses will be described. Using the *DIA* (Debris Impact Analysis) option each fragment is defined by an associated ballistic coefficient and final geometric cross section. Furthermore a single breakup altitude and a common ballistic coefficient applied to the re-entry before breakup has to be specified, i.e. up to the specified breakup altitude the trajectory of the parent object is propagated. From the breakup point on, one trajectory for each ballistic coefficient is propagated. Since this analysis provides no information on the shape and size of the impact objects, but this information is required to calculate the human risk, the user has to specify the final cross section for each fragment.

Another method that analyses a destructive re-entry is implemented in the DARS (Debris Analysis for Re-entry Spacecraft) module. DARS is a tool developed by ESA (ESTEC), but has been made available as an optional ASTOS module. Through a trajectory propagator and an aerothermodynamics module, DARS supplies the ephemeris and the thermal state of each fragment. It is able to determine if the object will reach the surface of the planet or if it will be burnt up on its path through the atmosphere. In case the object reaches the surface of the planet, DARS computes the kinetic energy at the impact point and provides the necessary data to perform the risk analyses for the re-entry (the probability of casualty and fatality). Additional output like shape and position of the footprint are generated by ASTOS. While propagating the trajectory DARS uses the environmental models of ASTOS, i.e. the atmospheric and gravitational models selected by the user.

DARS calculations are based on a simplified geometric model: the user can select from a set of primitive shapes like sphere, box, plate and cylinder. The fragmentation history and explosion events are either user-defined or triggered by events like the excess of a critical temperature or a certain percentage of melted material. Fragments are either user-defined or they are created by a parameterized stochastic explosion model. Besides the geometry the user must specify the initial mass, initial temperature and the material for the parent and for each user-defined fragment. The shape, size, mass and induced velocity of automatically created fragments is defined by the explosion model.

User-defined fragments may have a final altitude. At the final altitude the propagation of the fragment trajectory

stops and its final position is used as initial state for all the objects that have been defined as child of this fragment. Further on these (child) fragments may have a final altitude greater than zero and further successors. In this way multiple break-ups are realized. Premature fragmentation may be triggered if a critical percentage of the object is melted.

DARS is using a lumped thermal mass model for the heating and melting process. This calculation is based on the user-provided material properties: specific heat capacity, specific melting heat, melting temperature and emissivity. Objects may be defined as sheltered by other objects, i.e. they are not heated until a pre-defined percentage of the sheltering object is melted. For each fragment the aerodynamics is calculated based on the shape and the current Mach number, assuming tumbling objects. The aerodynamics of the parent object before the first breakup is defined by ASTOS.

The output of DARS is the trajectory of each fragment, its final impact location (if not burnt up before), its projected area, final velocity and final mass. With this output the calculation of risk figures may be performed in the same way as described in the ballistic analysis section.

2.1.3. Explosion Modelling

The idea behind the explosion model is to provide statistical information about the number of fragments created by the explosion, their area-to-mass distribution and their velocity distribution. This stochastic data is used to populate the fragments table of DARS.

The explosion model is derived from [2].

According to [2] the number of explosive fragments N of size L_c or larger (L_c provided in meters) is governed by the equation

$$N(L_c) = 6pL_c^{-1.6} \quad (1)$$

where p is a parameter that depends on the scenario, i.e. the size and type of the re-entering object. Fig. 2 shows a typical number distribution.

The area-to-mass distribution of the explosion fragments is defined as

$$D_{A/M}(L_c, \chi) = \alpha N_1 + (1 - \alpha)N_2 \quad (2)$$

where χ represents the distribution variable

$$\chi = \log_{10}(A/M) \quad (3)$$

and N_1 and N_2 the normal distribution function

$$N_{1/2} = \left[\frac{1}{\sigma_{1/2}(2\pi)^{0.5}} \right] e^{-\frac{1}{2} \left(\frac{\chi_{1/2} - \mu_{1/2}}{\sigma_{1/2}} \right)^2} \quad (4)$$

where α , μ_1 , μ_2 , σ_1 , σ_2 are parameters that depend on the characteristic length L_c and on the type of re-entry.

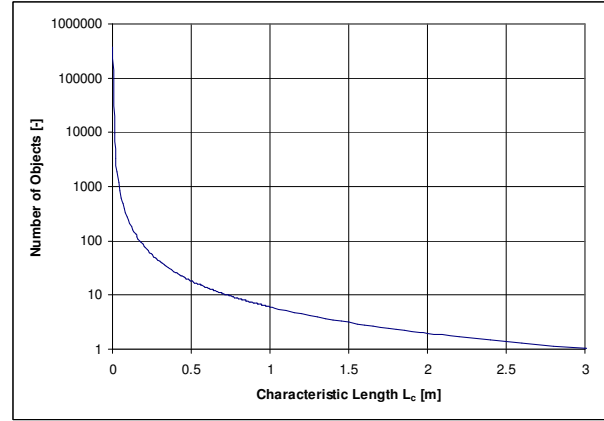


Figure 2. Typical number distribution of explosion fragments

According to [2] the above mentioned distribution is valid for objects larger than 11 cm. For objects smaller than 8 cm, the simpler function

$$D_{A/M}(L_c, \chi) = N(L_c, \mu_s, \sigma_s, \chi) \quad (5)$$

is used, where N is again the normal distribution function with parameters μ_s , σ_s depending on the characteristic length L_c . In the intermediate regime between 8 and 11 cm, a bridging function has to be used.

Following the assumptions made in [2] the mass of each fragment can be derived from its area-to-mass ratio A/M

$$M = A_x / (A/M) \quad (6)$$

where A_x is a function of the characteristic length L_c . Moreover the distribution of the velocity increment is identified as a function of the area-to-mass ratio:

$$D_{\Delta V} = \left[\frac{1}{\sigma_{\Delta V}(2\pi)^{0.5}} \right] e^{-\frac{1}{2} \left(\frac{v - \mu_{\Delta V}}{\sigma_{\Delta V}} \right)^2} \quad (7)$$

where

$$\begin{aligned} v &= \log_{10}(\Delta V) \\ \mu_{\Delta V} &= 0.2 \log_{10}(A/M) + 1.85 \\ \sigma_{\Delta V} &= 0.4 \end{aligned} \quad (8)$$

With the abovementioned continuous distribution functions for the number of objects, the area-to-mass ratio and the velocity increment the fragment table of DARS could not be filled. In order to do that, the continuous distributions need to be transformed into classes of objects of a certain characteristic length and area-to-mass ratio. Iteratively the parameter p in Eq. 1 needs to be adapted to fit the total mass of the fragments.

Afterwards each class is split into subclasses with a certain velocity increment (according to the distribution function).

To complete the definition of a fragment, its material and shape needs to be defined. Therefore the user has to specify the material composition of the parent object. Then the materials are assigned to the fragments in a way that fits best the user-defined material distribution.

For the type of shape a uniform distribution is assumed. In case of spheres the characteristic length defines already the geometry, in all other cases a ratio between the diameter and the length or the height and the length is required. For plates and boxes a second ratio is required. Both ratios are uniformly distributed. The bounds of these ratios are specified by the user.

2.2. Risk Estimation

Based on the final geometry, kinetic energy and on the calculated impact points, the risk for humans due to each individual object and an overall risk value is computed. Besides the risk for people on-ground, an assessment for the imposed risk for planes and ships are provided. In the following the assessment approach is detailed.

Based on the trajectory and the final geometry of each fragment a casualty cross sections A_C according to NASA Safety Standard NSS1740.14 [4] is calculated:

$$A_C = \left(\sqrt{A_h} + \sqrt{A_F} \right)^2 \quad (9)$$

where A_h is the projected area of the risk imposed target, and A_F is the projected area of the fragment (final cross sections).

2.2.1. On-ground Risk

For on-ground humans $A_h = 0.36 \text{ m}^2$ is assumed, which represents a standing person that is hit vertically. The on-ground risk calculation is based on the GPW V3 population density model [11]. Population growth is considered by an exponential growth rate assumption.

The calculation of risk values is similar to the method described in [3]. In order to consider uncertainties, the atmospheric density above the break-up is varied by $\pm 20\%$ and an additional impact uncertainty of ± 40 kilometres in cross range direction is assumed. The resulting impact swath and the nominal impact may be

plotted with the integrated plotting tools of ASTOS (see Fig. 3).

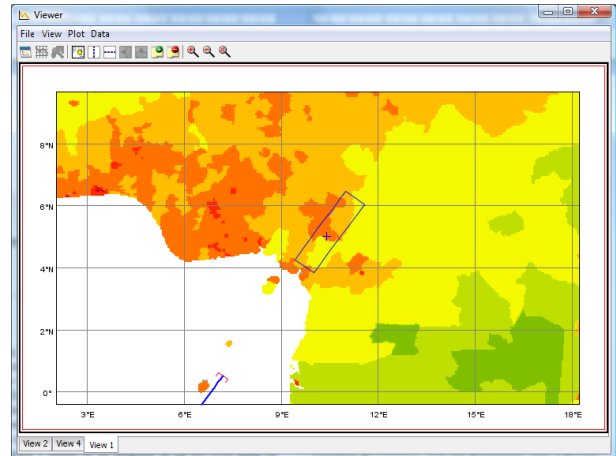


Figure 3. Impact swath and nominal impact plotted by ASTOS

Looking closer to the human risk analysis, it is required to distinguish between the probability to hit someone (casualty probability) and the probability that a person will be killed by a fragment (fatality probability). Typically small fragments with small kinetic energy (below 15 Joule) will not kill a person even if it hits him directly. The fatality probability is computed from the casualty probability and the kinetic energy of the fragment. It is defined as the casualty probability times the fatality index, whereas the fatality index is a dimensionless quantity between 0 and 1. Its value against the kinetic energy is shown in Fig. 4.

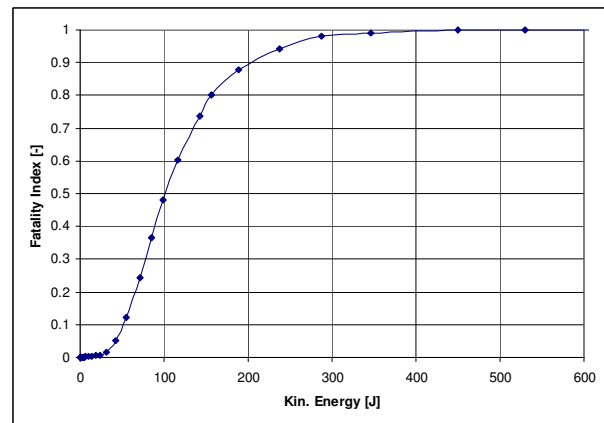


Figure 4. Fatality index vs. kinetic energy [12]

2.2.2. Maximum Probable Loss

Besides the risk to hurt or kill a person often the risk of financial loss is of interest. Maximum probable loss (MPL) is a risk-based analysis that yields the greatest potential loss, for bodily injuries and property damages that can reasonably be expected to occur as a result of licensed launch or re-entry activities.

In a first step an area is identified that will contain all

the impacts from debris resulting from any possible mishap, to within the 10^{-7} probability threshold. In other words, the probability of any debris falling outside the identified area is smaller, or more remote, than the 10^{-7} threshold. To allow for external probabilities that are not covered by the analysis, a user-defined base probability may be specified that is multiplied with the probability of each impact location.

Within the identified area the MPL methodology determines a monetary value to the estimated casualties, the loss of property, the loss of use, and the environmental damages and clean up costs that are expected. In particular, casualties are assigned a user-defined monetary value. The MPL methodology is described in detail in [8]. In contrast to the approach described in [8], individual high-value assets are not considered in ASTOS, but the provided threshold area may be used to find relevant high-value assets. However, the MPL methodology assumes somehow a worst-case scenario, e.g. instead of the mean population density data for grid bins of $2.5^\circ \times 2.5^\circ$ (as used for the on-ground risk assessment) a maximum population density value is used to calculate the number of casualties. The user needs to specify the following values (defaults in brackets):

- the monetary ‘value’ of each casualty (3.5M€)
- property loss as percentage of casualty loss (50%)
- the costs for environmental damage and cleanup (70,000€)

With the ASTOS Batch Mode Inspector (see section 2.3) a Monte Carlo analysis may be performed to identify the worst-case scenario within the scenario and the 10^{-7} threshold.

2.2.3. Risk for Airplanes

ASTOS calculates the risk that an airplane is hit by a re-entering object and also the casualty and fatality probability for the passengers.

The underlying traffic density data is derived from tracking data, i.e. a lot of flights were archived to identify the variation of their flight routes. Fig. 5 shows the recorded flights for one selected route.

It had been identified that the variations are quite large and not following a well describable distribution. Due to the jet stream seasonal variations can be observed, but there are a lot of exceptions probably caused by local weather conditions, why no statistical assumptions could be derived from the tracking data. Instead a different approach was taken. For each region (Atlantic, Pacific, USA continental, ...) and season a bandwidth to the north and to the south of the great circle arc has been identified. For a large time span each flight (departure and arrival airport) has been collected according to the flight plan.

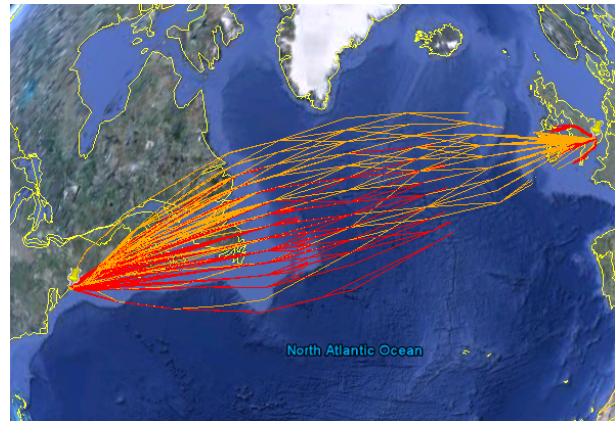


Figure 5. Tracked flights between two airports

Instead of using the real tracking data (that was also not always available) the great circle arc and the above mentioned regional bandwidths were used as basis for the following preparations. In the vertical plane a variation of 5,000 meters has been assumed.

The locations of the departure and arrival airports and the maximum variation (bandwidth) that is applied in the middle of the arc form an ellipse-like shape.

These shapes were created for each flight in the flight plan. The area within each shape represents one airplane within the total time span of the analysed data (somewhere in the shape). Together with the local cross-range extension the probability that the analyzed plane is located within a given volume may be derived.

Fig. 6 shows a graphical representation of this traffic density. In opposite to Fig. 5 only one flight direction from UK to the USA is shown.

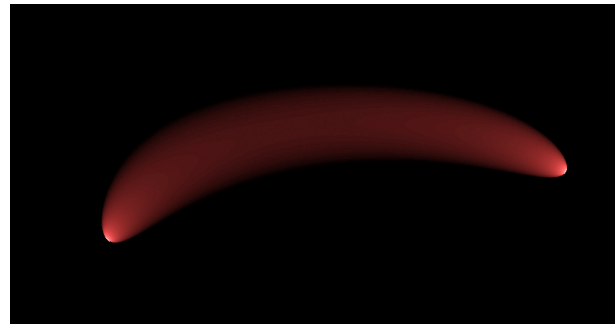


Figure 6. Traffic density for a single flight route

Repeating the last steps for all flights from the flight plans allows generating an air traffic density map as illustrated in Fig. 7. These traffic density maps were created for all four seasons. Based on the traffic density data three different probabilities are calculated:

- The probability to hit a plane
- The probability of a casualty
- The probability of a fatality

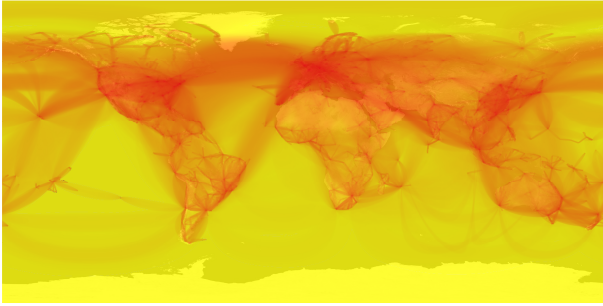


Figure 7. Air traffic density

As a first step the casualty area has to be calculated (see Eq. 9). Since the velocity of the fragment is small with respect to the plane, a frontal impact may be assumed. For the probability that the plane is hit a total frontal area of 60 m^2 is assumed, which reflects a typical intercontinental airliner.

For the probability of a casualty or fatality two different scenarios must be considered: either the plane is hit and it crashes or a passenger is directly hit by a fragment.

For both cases different reference areas will be applied: For the first, again the total frontal area of the plane is used, for the second 4 m^2 , which reflects the body area of 8 people sitting in one row, is assumed.

The probability of an impact is scaled by a crash index that depends on the kinetic energy of the fragment. This crash index may have values between 0 and 1. The product is the probability for a crash, which is also assumed as the probability for a casualty and also for a fatality.

The direct hit of a person could cause a casualty or even a fatality. Once again the fatality index described in section 2.2.1 is applied, but the kinetic energy, which is a parameter of this fatality index, is reduced by the energy required to penetrate the skin of the plane. This energy depends of course on the size and shape of the object, why a constant specific energy, i.e. the energy per cross-section area is used.

The requirement EASA CS25.631 [9] says that the plane must resist an impact of a 4 lb chicken at sea level cruise speed or at 0.85 times cruise speed in 8000 ft altitude. For typical airliners this corresponds to a kinetic energy of around 27 kJ. Assuming a reference area of 78 cm^2 this corresponds to a specific energy of 3.4 MJ/m^2 . This value is used for the reduction of the kinetic energy that impacts the passenger.

Comparing the probabilities for casualty or fatality due to a crash and the probabilities due to a direct impact, only the larger value will be reported.

2.2.4. Risk for Ships

The risk assessment for ships is based on data taken from [7] (see Fig. 8). The figure shows the track of 3,374 ships that were recorded for a period of one year. This number represents 11% of the 30,851 merchant ships >1000 gross tonnage at sea in the year 2005. The colour range in Fig. 8 represents the number of ships

that were recorded within a 1 km^2 bin (blue = 1, red = 1,158 ships) in the period of one year.

Before the data might be used for risk assessment it need to be generalized, i.e. the individually tracked routes must be transformed to generalized traffic density information. Therefore the values had been blurred (smoothened) depending on the distance from the next land mass (next to the coast and next to harbours the variations are usually smaller).

As reference area for the casualty area $20,000 \text{ m}^2$ is used. This value belongs to a relatively large and modern containership so that the resultant probabilities will be a conservative estimation.

The output of this assessment is the probability to hit a ship. Probabilities for casualties or fatalities are not calculated.

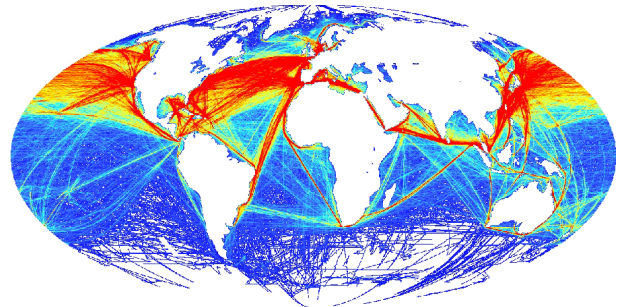


Figure 8. Global ship traffic [7]

2.3. ASTOS Batch Mode Capabilities

As shown in section 2.2 most of the time it is required to perform some kind of Monte Carlo analysis to reflect the uncertainties in the models and in the environmental conditions.

For this purpose ASTOS comprises a tool called "Batch Mode Inspector" that enables the user to perform Monte Carlo analyses without third-party tools and to plot the results directly by means of ASTOS plotting capabilities. The user can associate a batch variable to each model uncertainty. Then, in the Batch Mode Inspector, he can build the structure of the processes with which the batch variables are used in order to run the model automatically over a given parameter space. The structure consists of various batch elements freely chosen by the user. These can be actions like *Initialize*, *Simulate*, *Optimize* or post-processing elements that prepare the data taken from the simulation for further analysis (see Fig. 9).

The batch variables may be modified by *Loop* and *Random* elements. *Loop* will change a batch variable monotonously from an initial value to a final value using a given increment. Instead with the *Random* element it is possible to compute random numbers with Gaussian or uniform distribution. Uniform distribution variables are defined by a lower and upper bound, Gaussian by their mean value and the standard deviation. Additionally it is possible to specify lower

and upper bounds for Gaussian-distributed random numbers; this is useful if a physical boundary shall not be exceeded.

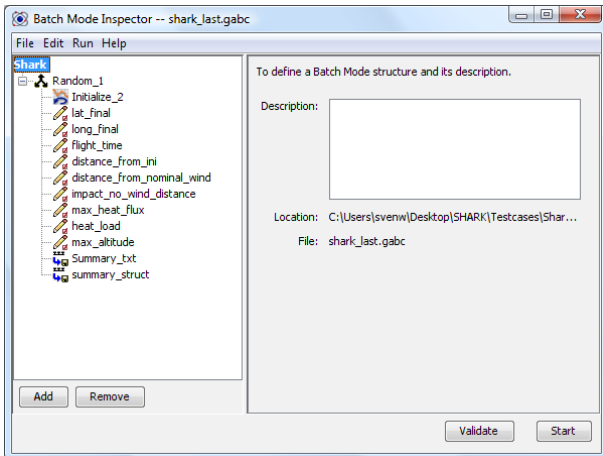


Figure 9. ASTOS Batch Mode Inspector

The Batch Mode Inspector is therefore ideal to perform Monte Carlo analyses on the impacting objects in order to produce a footprint of them like the one shown in Fig. 10.

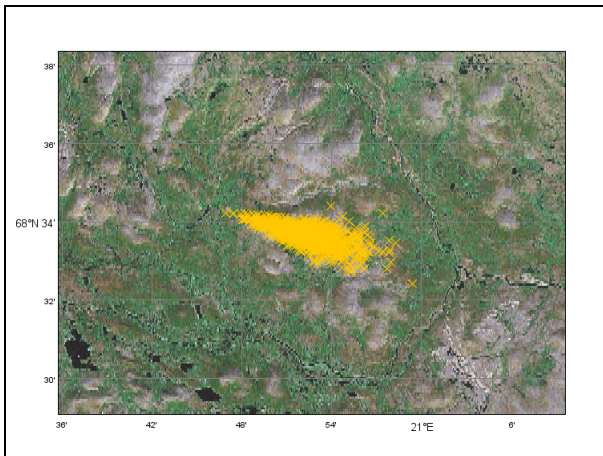


Figure 10. Result of a Monte Carlo analysis made with ASTOS and its Batch Mode

3. IN-ORBIT RISK ASSESSMENT

ASTOS comprises an optional module called CAM (Conjunction Analysis Module) that allows the calculation of close encounters between the simulated vehicle and objects taken from the NORAD catalogue [10].

The NORAD catalogue contains mean orbit data for several thousands of objects: operational satellites, burnt stages and other debris. The orbit data is stored in the Two-Line-Element (TLE) format.

In order to calculate the nominal distance between the simulated vehicle and an object from the catalogue both trajectories need to be propagated. These propagations need a lot of time, so it would improve the performance

if objects from the catalogue could be identified as non-critical without propagating their trajectory.

Looking at the perigee and apogee of the catalogued object and the vehicle, objects may be identified that never cross the trajectory of the vehicle because they fly in different altitude regimes. To improve this filtering approach the trajectory is split into several arcs. The trajectory is split and a new arc is created when either the perigee or apogee crosses a boundary value. Parts of the trajectory, where the current altitude is below 85 km, will be completely neglected.

Each arc is analysed separately. Since the arcs have a narrow radius range a lot of objects may be filtered from the catalogue. A trade-off had been made to find the number of distinct radius regimes that provides typically the best performance.

Another filtering criterion is the orbit inclination of the catalogued object. If the declination range of the vehicle in the current arc is larger than the inclination of the object (looking at the absolute values), the object may be filtered. This filter is not as effective as the perigee and apogee filter since only very few arcs have such a small range of declination. Therefore additional arc splitting is introduced when the declination passes $+65^\circ$ or -65° .

Up to this point the above mentioned procedure has not considered any uncertainties in the catalogue data. In reality there might be objects identified as non-critical which will come very close even cause a collision just because their orbit data was only roughly known and the real trajectory was far away from the nominal calculated with the mean orbit parameters.

Unfortunately uncertainty information is not provided by NORAD. Therefore the history of orbit data provided for each object has been analyzed:

For burnt-stages, inoperative satellites and debris the variation of orbit data is taken as measure for the uncertainty of their orbits. These uncertainties will not be applied to each individual object, but the objects from the catalogue are divided into classes. Within one class the mean uncertainties are applied.

A class is defined by the type of object, the nominal orbit inclination, eccentricity and semi-major axis.

Depending on the difference between simulation time and the TLE epoch, margins are applied to the filtering process. Furthermore the uncertainty in position that is estimated from the uncertainty in the TLE data is considered when characterising objects as critical.

The impact probability of each critical object is then derived from a Monte Carlo analysis. Output of the Monte Carlo analysis is the variation of the minimum distance, i.e. the worst case variation in distance is obtained for a 1-sigma probability ellipsoid. Considering a normal distribution the probability to hit the vehicle can be directly derived by scaling the ellipsoid to a size where the minimum distance may become zero (here the size of the vehicle is considered). Doubling the size would refer to a 2-sigma ellipsoid,

tripling the size refers to a 3-sigma ellipsoid and so on. If a 3-sigma ellipsoid is required to achieve the zero distance, it means that the impact probability is 0.27%. Thus, impact probabilities may be easily derived.

4. CONCLUSION

ASTOS comprises a wide range of risk assessment methodologies that is continuously extended. From early design phases till operations ASTOS may be used for risk assessments.

Due to its flexibility it can even comply with local, non-common safety guidelines and procedures.

A lot of future developments are planned, e.g. the extension of CAM to a tool that can predict also close encounters between two objects from the NORAD catalogue. The risk assessment for ship traffic shall be extended to provide also casualty probabilities.

5. REFERENCES

1. Wiegand, A. et al. (2009), *ASTOS User Manual*, Version 6.1.2, Astos Solutions GmbH, Unterkirnach, Germany.
2. Johnson, N. L., Krisko, P. H., Liou, J.-C., Anz-Meador, P. D. (2001), NASA's New Breakup Model of Elove 4.0, COSPAR, *Adv. Space Research*, Vol 28, No. 9, pp. 1377-1384.
3. Klinkrad, H., Fritsche, B., Lips, T. (2004). A Standardized Method for Re-entry Risk Evaluation, *Proceedings of the 55th International Astronautical Congress*, Vancouver, Canada.
4. anon. (1995). *NASA Safety Standard: Guidelines and Assessment Procedures for Limiting Orbital Debris*, NSS 1740.14, Houston, USA.
5. Lips, T. et al. (2005). Comparison of ORSAT and SCARAB Reentry Survival Results, *Proceedings of the 4th European Conference on Space Debris*, Darmstadt, Germany.
6. Wiegand, A. et al. (2009). *ASTOS Model Library*, Version 6.1.2, Astos Solutions GmbH, Unterkirnach, Germany.
7. Halpern, B. et al. (2008). A Global Map of Human Impact on Marine Ecosystems. *Science*, Vol. 319. no. 5865, pp. 948 - 952
8. anon. (2002). *Maximum Probable Loss Methodology*. 2nd edition, Australian Government, Space Licensing and Safety Office, Australia.
9. anon (2003). *Certification Specifications for Large Aeroplanes CS-25*. ED Decision 2003/2/RM, European Aviation Safety Agency, Cologne, Germany
10. United States Strategic Command (USSTRATCOM). Space-Track – The Source for Space Surveillance Data. Online at <http://www.space-track.org>.
11. Center for International Earth Science Information Network (CIESIN), Columbia University; and Centro Internacional de Agricultura Tropical (2005). *Gridded Population of the World Version 3 (GPWv3)*. Palisades, NY: Socioeconomic Data and Applications Center (SEDAC), Columbia University.
12. US Army White Sands Missile Range (2000). *Common Risk Criteria for National Test Ranges – Inert Debris*, Standard 321-00 (US)